SEECCM III
3rd South-East European Conference on Computational Mechanics-
an ECCOMAS and IACM Special Interest Conference
M. Papadrakakis, M. Kojic, I. Tuncer (eds.)
Kos Island, Greece, 12–14 June 2013

MULTISCALE MODELING OF MOLECULAR DIFFUSION IN TISSUE

Miljan Milosevic[1], Milos Kojic[1, 2], Nikola Kojic[3], Mauro Ferrari[2] and Arturas Ziemys[2]

[1] Belgrade Metropolitan University - Bioengineering Research and Development Center BioIRC
Prvoslava Stojanovica 6, 3400 Kragujevac, Serbia
e-mail: miljan.m@kg.ac.rs

[2] The Methodist Hospital Research Institute, The Department of Nanomedicine
6670 Bertner Ave., R7-116, Houston, TX 77030
e-mail: mkojic@hsph.harvard.edu, mferrari@tmhs.org, aziemys@tmhs.org

[3] Center for Engineering in Medicine and Surgical Services, Massachusetts General Hospital
Harvard Medical School, Boston, MA 02114
e-mail: kojic@mit.edu

Keywords: diffusion, hierarchical modeling, complex media, microstructural model, equivalent continuum model, numerical homogenization.

Abstract. *Tissue can be considered as a composite medium through which occurs transport of molecules. Transport of matter by diffusion within this medium is affected not only by internal microstructural geometry, but also by physico-chemical interactions between solid phase (proteins, fibers) and transported molecules or particles. We implement a new hierarchical multiscale microstructural model [1], [2] for simulation of transport of molecules through tissue. Our model is based on a novel numerical homogenization procedure. The equivalent diffusion parameters of the continuum model consist of equivalent bulk commonly used diffusion coefficients and new equivalent distances from the solid surface. Numerical examples include, among others, a model of diffusion within tissue in the vicinity of a capillary through which molecules are transported by convection. A study of the effects of collagen mesh density within tissue on transported molecule concentration profiles is presented.*

1 INTRODUCTION

Classical continuum theories of diffusion through homogenous media are based on Fick's law:

$$J = -D\nabla c \tag{1}$$

where $\boldsymbol{J}$ is the mass flux along concentration gradient ∇c with diffusion coefficient (diffusivity) D. However, in complex media, phase interface may occupy a substantial portion of diffusion domain so that diffusion transport is affected by molecular interactions with the surface, and predictions following equation (1) may become inaccurate. MD (molecular dynamics) modeling and experiments have shown that diffusive transport of molecules and particles in nanochannels is affected by their proximity to a solid surface [3], [4]. Using MD analysis, it is shown in [3] that molecular diffusivity depends on both concentration and confinement effects. Therefore, modeling of these transport regimes needs novel approaches that could bring molecular scale information into complex macroscale models of nanofluidic devices. An ideal scenario is to properly transfer MD information to macroscopic models. Hierarchical (multiscale) modeling approach, introduced in [1] and which couples MD and Finite Element Method (FEM), offer this possibility.

Here, we will introduce a multiscale hierarchical model for diffusion at the microstructural level (further termed as 'microstuctural model'), within a small reference volume (RV), Figure 3b. The implemented method is effective, robust and generalizable to a variety of problems where diffusion governs transport. Further, we formulate a 'continuum' model which employs the results obtained by the microstructural model for diffusion within the RV. Our method relies on the fundamental condition of the equivalency of mass-release kinetics between the continuum and microstructural models for a given region of space and over a prescribed concentration range. The continuum model is based on constitutive parameters, which include equivalent 'bulk' diffusion coefficients (characterizing free, or Fickian, diffusion within the solvent) and equivalent distances from an imaginary surface (describing surface effects within the microstructure, [1]). Constitutive parameters, depending only on the structural geometry and the material properties of the diffusing constituents, are evaluated for three orthogonal coordinate directions – enabling modeling of general 3D diffusion conditions.

2 METHODS

2.1 MD simulations and scaling function for diffusion coefficient

Molecular Dynamics (MD) has been used for several decades [5]. It is based on statistical mechanics, where motion of particles is described according to the Newtonian mechanics:

$$m_i \dot{\mathbf{v}}_i = \mathbf{F}_i \tag{2}$$

where m_i, $\dot{\mathbf{v}}_i$ and $\mathbf{F}_i$ are mass, acceleration and resulting force (including interaction forces from the neighboring particles and external forces), respectively. The interaction forces include bonded (repulsive-attractive, bending and torsion) and non-bonded (electrostatic, van der Waals) terms. The Force Field (FF) represents a functional form of behavior of chemical structures and is evaluated from potential energy function, $E = E_{intra} + E_{inter}$, of CHARMM FF [6] which is used in our MD models. MD simulations for calculating diffusion coefficients in nanochannels were carried out [1],[7] using NAMD 2.6 [8] with a TIP3P water model [9] and NVT (fixed number of particles N, pressure P, volume V) ensembles. CHARMM compatible amorphous silica force field [10] was employed to model the silica nanochannel, which is

modeled by charged hydrophilic amorphous silica phase to match the silica properties after the fabrication process. Glucose diffusion coefficients were calculated from 30 ns trajectories by using the mean square displacement $<r^2>$:

$$<r^2>=2dDt \tag{3}$$

where the factor d = 1, 2, 3 depends on the dimensionality of the space, and t is time. The diffusivity along the surface normal (z-direction) was evaluated, from the surface up to the middle of the nanochannel. The diffusivity results include dependence on distance from the wall and glucose concentrations (Figure 1A).

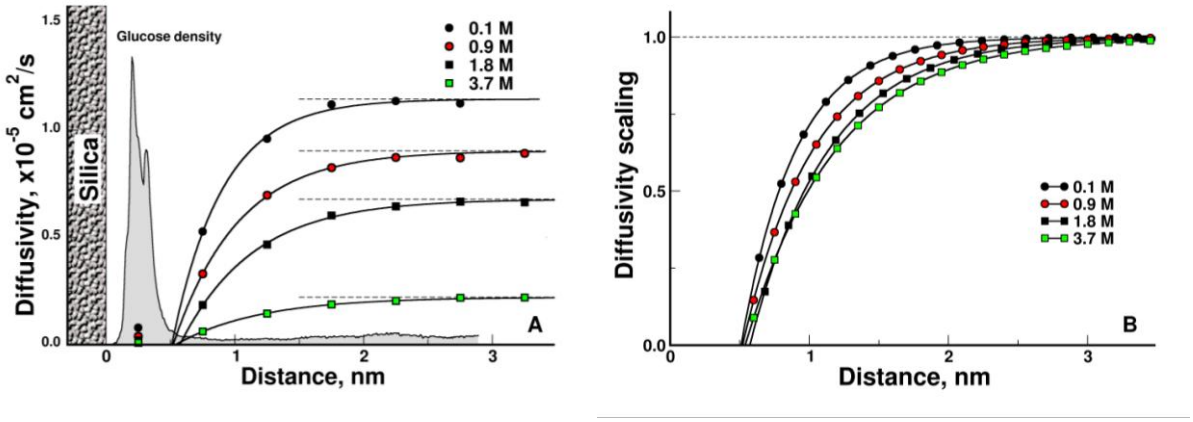

Figure 1: a) Calculated glucose diffusivity and b) scaling functions of the proximity to the silica surface for several concentrations; according to [1].

The MD calculated diffusivity is normalized with respect to the "bulk" value D_{bulk} corresponding to diffusivity far from the surface, where influence of the surface is negligible. Hence, we have:

$$D = SD_{bulk} \tag{4}$$

where:

$$S = S\ \ h,c\ \ , \quad 0 \le S \le 1 \tag{5}$$

is the scaling function which depends on the distance from the wall surface h and concentration c. Calculated scaling function is shown in Figure 1B.

Experimental investigations showed that $D(\equiv D_{bulk})$ for glucose depends on concentration, although data are quite different (see [1] and references given therein). For examples shown here we have chosen the glucose D according to the largest data set of [11] that spans over a wide range of concentrations, from 0 to 3.36 M, with linear dependence D(c).

2.2 Finite element model

We here consider unsteady diffusion where the diffusion coefficient depends on both concentration and spatial position of a point within the model. FE solution procedures for nonlinear diffusion problems have been well established and successfully used in various applications (e.g. [12],[13],[14],[15]). The basic mass balance equation, which also includes Fick's law in equation (1), is transformed into the incremental-iterative system of linear balance equations for a finite element [15]:

$$\left(\frac{1}{\Delta t}\mathbf{M} + {}^{n+1}\mathbf{K}^{(i-1)}\right)\Delta\mathbf{C}^{(i)} = {}^{n+1}\mathbf{Q}^{S(i-1)} + {}^{n+1}\mathbf{Q}^{V(i)} - {}^{n+1}\mathbf{K}^{(i-1)}\,{}^{n+1}\mathbf{C}^{(i-1)} - \frac{1}{\Delta t}\mathbf{M}\;{}^{n+1}\mathbf{C}^{(i-1)} - {}^{n}\mathbf{C} \tag{6}$$

where $\mathbf{C}$ is the vector of nodal concentrations; the left upper indices n and n+1 denote values at the start and end of the time step n of size Δt; the indices i and i-1 correspond to the current and previous equilibrium iteration; $\mathbf{Q}^S$ and $\mathbf{Q}^V$ are surface and volumetric nodal fluxes for the element; and components of the matrices $\mathbf{M}$ and $\mathbf{K}$ are:

$$M_{IJ} = \int_V N_I N_J dV \tag{7}$$

$${}^{n+1}K_{IJ}^{(i-1)} = \int_V {}^{n+1}D^{(i-1)} N_{I,i} N_{J,i} dV \tag{8}$$

Here N_I and N_J are the interpolation functions, and ${}^{n+1}D^{(i-1)}$ is the diffusion coefficient corresponding to the last known concentration ${}^{n+1}c^{(i-1)}$ at a point within the finite element. Assembly of equations (6) and solution procedures are performed in a usual manner that is well described in the computational mechanics literature (e.g. [12]).

In our models we have incorporated concentration and interface effects, according to equation (4) into the FEM model. Implementation of the expression (4) is illustrated in Figure 2. Note that linear interpolation between scaling curves is used.

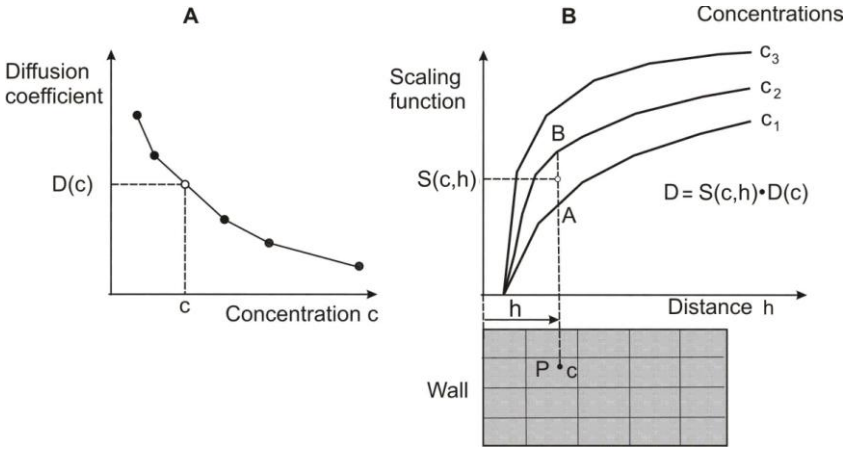

Figure 2: Determination of diffusion coefficient at a spatial point P using dependence on concentration and surface effects. The "bulk" value is first determined from the curve D(c), A; then the scaling function is evaluated form family of curves shown in B. Linear interpolation curves S(c,h) is adopted (between points A and B in the figure); according to [16].

2.3 Generalization of the hierarchical model to porous media

Here we outline a generalization of the hierarchical model to diffusion in complex porous media, consisting of distributed solid constituents within fluid. For simplicity of presentation of this generalization, we assume a medium with solid fibers, as sketched in Figure 3.

The main idea here is to determine equivalent diffusion parameters of a homogenous porous medium which capture the internal structure of a composite medium in a way that diffusion properties are preserved. To achieve this, we first take a reference volume around a

material point (in a form of a cube) around that point, Figure 3a, and discretize it into finite elements (Figure 3b).

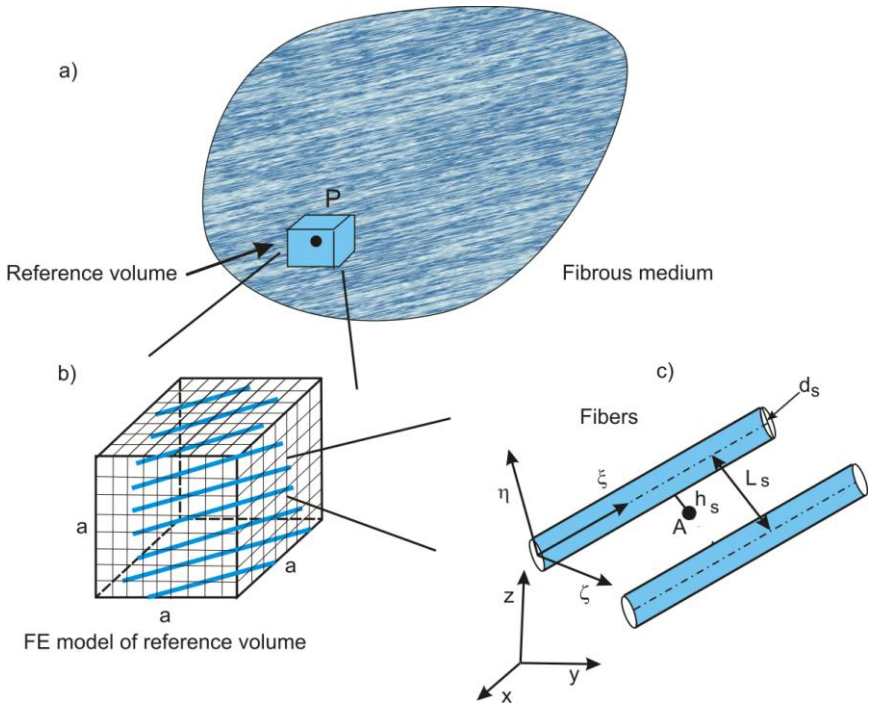

Figure 3. Concept of extension of hierarchical model to porous medium with fibers. a) Fibrous medium with reference volume at a material point P; b) Reference volume discretized into finite elements; c) Geometry of the internal structure – fibers of a s-group, with diameter d_s and with mutual distance L_s, and point A at distance h_s from the fiber surface.

Here we take the real internal microstructure and calculate diffusion in three orthogonal directions. In this FE model it is possible to properly take into account the surface effects, as sketched in Figure 3c. Namely, for a point A in the medium we calculate distance from the closest fiber surface of an s-group, and evaluate scaling function S_s as described above for diffusion within a nanochannel. We assume that scaling functions are different for the normal and tangential directions, hence we have three scaling functions S^s_ξ, S^s_η, S^s_ζ in the local fiber directions ξ, η, ξ, so that the diagonal diffusion matrix (tensor) $D^s_{\xi\xi}, D^s_{\eta\eta}, D^s_{\varsigma\varsigma}$ in the local coordinate system is:

$$\begin{aligned} D^s_{\xi\xi} &= S^s_\xi D_{bulk} \\ D^s_{\eta\eta} &= S^s_\eta D_{bulk} \\ D^s_{\varsigma\varsigma} &= S^s_\varsigma D_{bulk} \end{aligned} \tag{9}$$

where D_{bulk} is the bulk modulus. The diffusion tensor in the global coordinate system x,y,z can be obtained by tensorial transformation of the second-order tensor:

$$\mathbf{D}^s_{xyz} = \mathbf{T}^s \mathbf{D}^s_{\xi\eta\varsigma} \mathbf{T}^{sT} \tag{10}$$

where the components of the transformation matrix contains cosines of angles between local and global axes:

$$T_{ij}^{s} = \cos(x_i, \xi_j) \qquad i,j=1,2,3 \tag{11}$$

Here x_i and ξ_j stand for global (*x*,*y*.*z*) and local coordinate (ξ, η, ς) systems.

2.4 Numerical homogenization procedure and continuum model

We introduce a novel numerical homogenization procedure to determine the appropriate diffusion properties of a continuum model with a given microstructure. The basic condition governing this procedure is the equivalence of mass fluxes (through any surface in the diffusion domain) for the microstructural and continuum model, at any time during diffusion process. Considering mass release curves for diffusion through an RV around a spatial point, we have that the mass flux J_i in direction x_i is given as:

$$J_i = \left(\frac{dm}{dt} \right)_i \tag{12}$$

This derivative is geometrically represented as the tangent to the mass release curve $m\ t_{\ i}$ for the direction x_i, therefore the fluxes are equal for both models if their mass release curves are the same. This interpretation of flux equality through an RV is analogous to the mass balance condition in a differential volume used in continuum mechanics.

Next, we calculate diffusion through the reference volume using equivalent quantities of a porous homogenous medium within the RV. The porosity *n* is evaluated from the internal structure of the RV. For each diffusion direction *i* (i.e. x,y,z), the steps are as follows:

1. Calculate mass release using initial diffusion using given $D_{bulk}\ \ c$.
2. Perform changes on the value D_0 until the mass release curve is close enough to the true curve, when the value is $\bar{D}_{0\ \ i}$.
3. Using $\bar{D}_{0\ \ i}$ calculate initial mass release curve taking into account equivalent values of the transformation matrix $\bar{\mathbf{T}}$ and equivalent distance from the solid surface $\bar{h}_{0\ \ i}$.
4. Search for the distance $\bar{h}_i$ when difference between the calculated and true mass release curves is within a selected error tolerance.

In the above calculations of the equivalent transformation matrix and initial equivalent distance $\bar{h}_{0\ \ i}$ a weighted procedure, which takes into account volumes belonging to FE nodes, is implemented (details not given here).

The presented concept of evaluation of parameters related to equivalent homogenous porous medium represents a numerical homogenization procedure. It can be extended to non-homogenous media, by varying equivalent parameters, or to stochastic characteristics. Application of introduced numerical homogenization method (NHM) is illustrated in the Results section.

3 RESULTS

3.1 Diffusion within agarose polymer solution

Here, we first present detailed analysis of the microstructural model and provide prediction of equivalent continuum model. We use the internal structure of the gel obtained by imag-

ing[17], shown in Fig. 4a with discretized agarose fibers, with a porosity of 97%. Fiber are discretized using "Agarose Fibers" interface software developed in BioIRC research and development center (Fig. 4b).

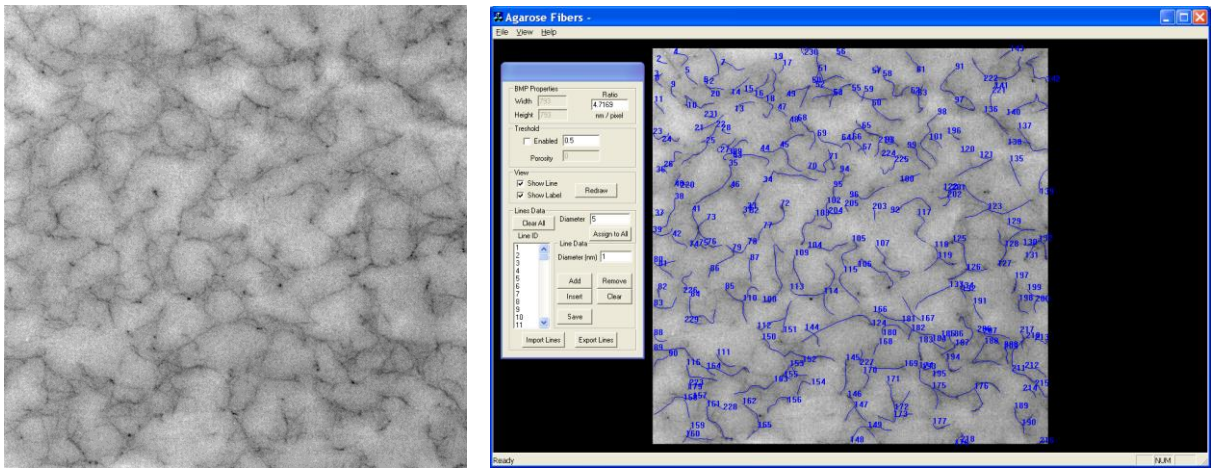

Figure 4. a) Internal microstructure obtained by imaging [17]; b) Fibers recognition software developed in BioIRC research and development center.

As expected, the calculated diffusion in the x and y directions are roughly equivalent, since the size of the RV (1,868 x 1.868 μm) is large enough so that the overall characteristics are the same in the two directions. Both microstructural and continuum models are used, giving the same total mass release.

In order to gain further insight into the diffusion within this polymer gel, we examine the mass flux and concentration distributions (Fig. 5a). Here, we consider the diffusion of molecules whose radius is 5 nm. The upper left panel shows the distribution of mass fluxes in the direction of diffusion at the end of the first time step, time t= 0.5 s. The field displays the variation of the flux due to the distribution of agarose fibers, with zero-values within the fibers and at the fiber surfaces. Diagrams of concentration and mass flux along the coordinate axes are shown in the lower-left and upper-right panels. Based on continuum solutions, the concentration decreases approximately linearly along horizontal line, and remains constant along vertical cross-section; flux-x is roughly constant along horizontal cross-section, and flux-y is equal to zero along vertical cross-section. On the other hand, microstructural solutions have variations, with zero-values at the points corresponding to fibers. Finally, the right lower panel shows both cumulative mass release and flux-x change in time during FEM simulation. Taken together, the continuum model incorporates the microstructural flux fluctuations in order to achieve an equivalence of mass fluxes between the microstructural and continuum models through a given RV.

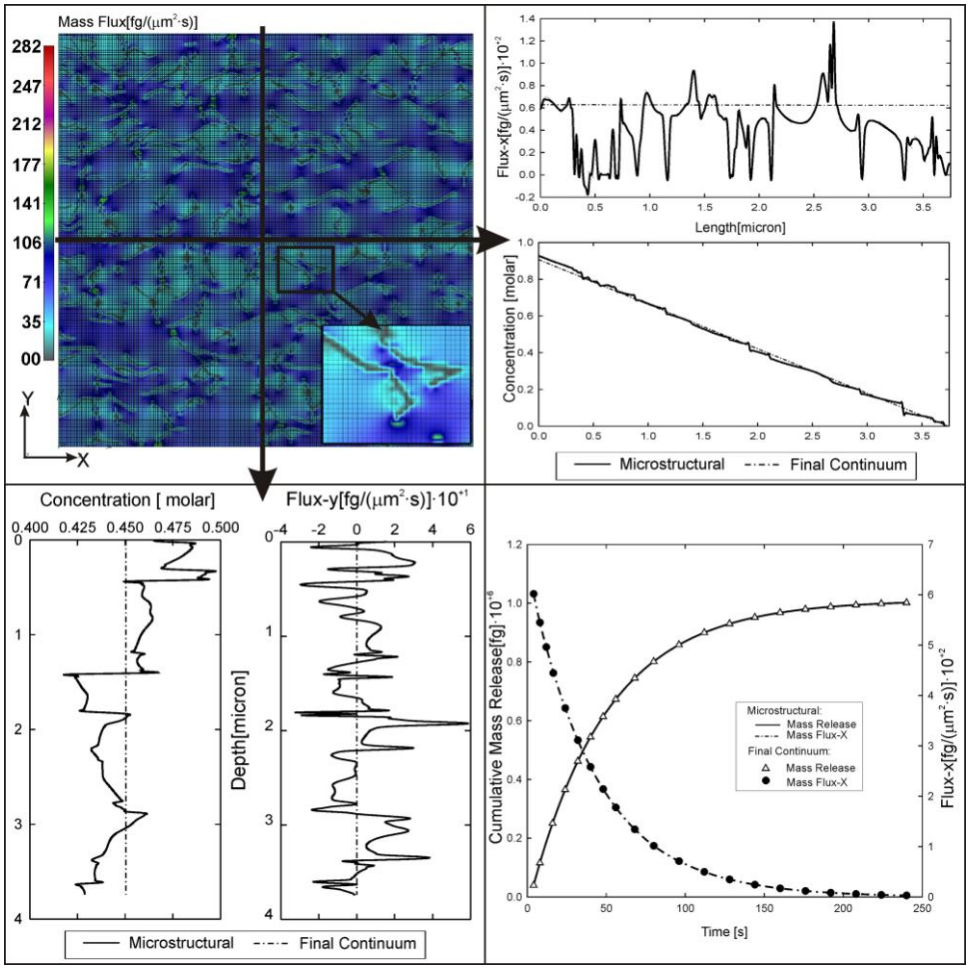

Figure 5. Diffusion within an agarose polymer gel. **Upper left panel**: Mass flux-x distribution at time t=0.5s; gray contours within the field shows zero-flux at fibers points. **Upper right panel**: Distribution of mass flux and concentration in the x-direction, microstructural (full line) and continuum (dashed line) along horizontal cross-section. **Lower left panel**: Distribution of mass flux and concentration in the y-direction, microstructural (solid line) and continuum (dashed line) along vertical cross-section. **Lower right panel**: Change of both cumulative mass release and flux-x in time for microstructural and continuum model.

3.2 Therapeutic particle transport across capillary wall

The space around a capillary is discretized as schematically shown in Figure 6. Due to axial symmetry, we use a part of the cylindrical domain defined by an angle (here it is 1/8 of full circle), as shown in Figure 6b. The diffusion space consists of two regions: a) sink domain corresponding to homogenous tissue medium, and b) sleeve domain which contains collagen fibers. The unsteady and nonlinear diffusion problem is solved in a standard manner, by employing incremental-iterative solution scheme [15]. Boundary conditions for the computational model are as follows: It is assumed that at the capillary surface concentration of molecules is constant over time, while far in the tissue (at the model external cylindrical surface) concentration is equal to zero.

Here we are exploring how structure of collagen, which is natural biological polymer constituting to structure of capillary walls, affects the diffusion of 80 nm liposome (PLD) and 1 nm size chemotherapeutic molecule doxorubicin (DOX).

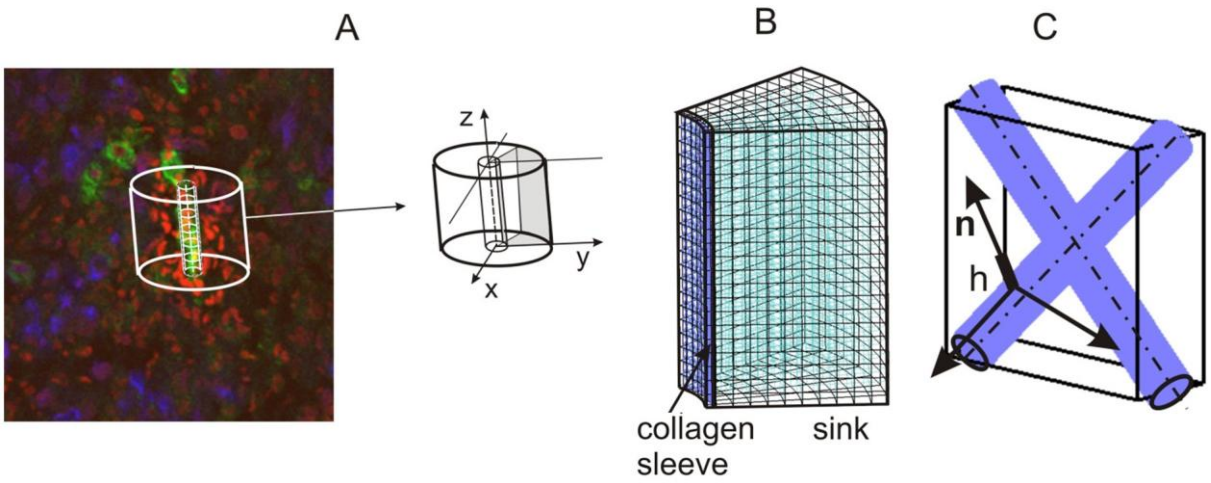

Figure 6. Finite element model: a) Schematics of the cylindrical diffusion domain around capillary and segment of the domain used in calculation. b) Finite element mesh for the collagen sleeve and sink regions. c) Finite elements with fibers; local coordinate system is used for evaluation of the diffusion coefficient, with *h* representing distance from the fiber surface along the normal **n** to the surface.

We have first formulated a microstructural hierarchical diffusion model, In order to investigate how collagen sleeve may control mass transport through capillary wall, we have created the collagen sleeve model that mimics a collagen surrounding capillaries [18-21]. For simplicity, particle concentrations inside and outside of a vessel were kept constant, and other structural elements of capillary wall were omitted to focus on collagen structural effects only. The later has real implication to drug penetration when endothelium cells are absent because of damage. We study the diffusion transport of liposomes and doxygen, different by size and physico-chemical properties, in response to different structures of collagen fiber mesh.

First, we investigate how surface effects affect mass diffusion by evaluating DOX and PLD mass release through collagen sleeve made of 3 mesh layers (each layer of thickness 10 nm) and adopting the following three assumptions: no fibers, fibers without surface effects, and fibers with surface effects on diffusion. It is taken that the concentration on the vessel surface is 0.02 M, while concentration at the outer surface of the sleeve is equal to zero, and both concentrations are kept constant over time.

Figure 7a compares diffusion mass transfer for all three cases and demonstrates the method. The differences of mass release between DOX and PLD in bulk (no fibers) are due to differences in diffusivity coefficients of particles. DOX mass release does not reveal substantial differences through 200 nm mesh in case with or without surface effects. That may be explained by small size of DOX molecule comparing to the openings in mesh (the ratio of the particle area projection to the tangential plane through which diffusion occurs, with respect to the pore area in the same plane, is $2.07 \cdot 10^{-5}$). PLD diffusion through collagen with 200 and 400 nm meshes not accounting for interactions with surface shows almost no differences, where the ratios of the particle area with respect to the pore area in the tangential plane are 0.0132 and 0.00323 respectively. However, the inclusion of surface effects makes a dramatic difference in PLD diffusion showing that smaller mesh openings will impede diffusion more and difference between 200 and 400 nm becomes substantial (Figure 7a). The inclusion of surface effects into the model also shows that diffusion mass transfer is strongly reduced when compared to mass release through the medium without fibers and using the classical Fickian diffusion law.

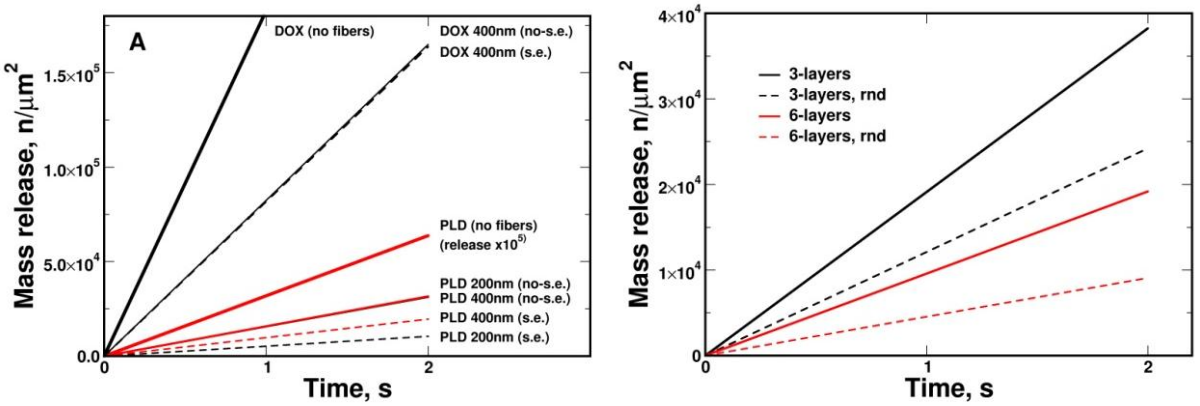

Figure 7. Fiber surface effects on diffusion. **a**) The effects of fibers and interface on DOX and PLD mass release through 3 collagen sheets of 200 and 400 nm mesh-size (*no-s.e.* – no surface effect; *s.e.* – with surface effects). b) Collagen mesh randomness significantly reduces the PLD mass release rate; random mesh solutions are displaced by dashed line.

Because the actual collagen mesh is not ordered structure and it is random, the effect of randomness was investigated. Figure 7b depicts mass release of PLD through 400 nm mesh having 3 and 6 mesh layers in a collagen sleeve, in case of ordered and randomized fiber composition. Randomized meshes showed significantly reduced mass release comparing to ordered meshes. For randomized mesh fluxes are approximately reduced by 30% in a 3-layers sleeve, and 50% in a 6-layer sleeve. Because DOX size is small comparing to mesh openings, there was no similar effect observed with DOX. Results show that randomized meshes may create larger obstruction for diffusion.

4 SUMMARY AND CONCLUSIONS

In summary, we have first formulated a microstructural hierarchical diffusion model, which includes surface interaction effects, for a general microstructural geometry. In this model, the interaction effects are incorporated through scaling functions (evaluated using MD), which represent the ratios between the real and bulk diffusion coefficients. The scaling functions, expressed in terms of distance from the solid surfaces and concentration, are calculated in the local coordinate system of the solid surface. Therefore, two domains of diffusion are distinguished: the bulk diffusion domain (with Fickian diffusion) and the domain near surfaces, with non-Fickian hindered diffusion. In both domains, diffusion is calculated by using the FE method. The surface effects become apparent when comparing the slower mass release kinetics (with surface interactions) with purely Fickian mass release (without surface effects).

This microstructural model is then employed within a novel numerical homogenization procedure to establish the equivalent continuum diffusion model. The procedure is general since it is applicable to an internal, structural geometry of any complexity, and can include different solid material sets with different material properties. The procedure relies on the condition that mass release curves of the two models must be equal. Constitutive diffusion parameters of the continuum model are determined for the three coordinate directions and include the traditional bulk diffusion coefficients, and also equivalent distances from the solid surfaces to account for surface interaction effects on diffusion. Furthermore, these constitutive parameters can depend on the local concentration. Our approach, consisting of a microstructural model and numerical homogenization procedure is general and robust, and offers new possibilities in modeling diffusion through complex materials, including molecular transport in biological systems (e.g. intercellular spaces and tissues). The presented methodology can

serve as a tunable platform for constructing intricate multiscale hierarchical diffusion models with additional complexity and effects, such as multiple molecule types (e.g. different proteins/ligands), multiple surfaces (e.g. various cell types with different receptors), and various media (e.g. different solvents). These multiscale models provide a basis for a deeper, more accurate representation of fundamental transport processes occurring throughout nature.

Numerical homogenization procedure presented in this work is analogous to homogenization procedures previously presented in linear and nonlinear solid mechanics, heat transfer and diffusion, where different types of RV were used (e.g. [22],[23],[24]). Previous homogenization procedures have limitations due to the special assumptions made regarding microstructure (e.g. periodicity) as well as relying on various asymptotic expansions of analytic forms. Our method is not only general, but also includes concentration-dependent parameters within a wide range of concentrations over which diffusion occurs.

By incorporating surface effects of polymer fibers into our recently developed multiscale diffusion model, it was found that DMX was free to diffuse through collagen sleeve containing 1 to 6 fiber meshes with mesh size 50 to 800 nm. However, LPS showed substantial decrease of flux through collagen sleeves of 3 mesh layers and smaller than 200 nm mesh sizes. This finding explains higher efficacy of particle-based drug carriers.

5 ACKNOWLEDGMENTS

This project has been supported with federal funds from NASA under the contracts NNJ06HE06A and NNX08AW91G, Department of Defense under the contract DODW81XWH-09-1-0212, as well as funds from State of Texas Emerging Technology Fund, Nano Medical Systems (NMS), Alliance of NanoHealth (ANH), and University of Texas at Houston. The authors acknowledge the Texas Advanced Computing Center (TACC) at The University of Texas at Austin for providing HPC resources that have contributed to the research results reported within this paper.

The authors acknowledge support from Ministry of Education and Science of Serbia, grants OI 174028 and III 41007, City of Kragujevac, and from FP7-ICT-2007 project (grant agreement 224297, ARTreat).

REFERENCES

[1] Ziemys A., Kojic M., Milosevic M., Kojic N., Hussain F., Ferrari M., Grattoni A. (2011). *Hierarchical modeling of diffusive transport through nanochannels by coupling molecular dynamics with finite element method*, Journal of Computational Physics, 230, 5722–5731.

[2] Kojic M., Milosevic M., Kojic N., Ferrari M., Ziemys A., Numeric modeling of diffusion in complex media with surface interface effects, Contemporary Materials, III-2, 153-166, 2012.

[3] Ziemys A., Grattoni A., Fine D., Hussain F., Ferrari M., *Confinement effects on monosaccharide transport in nanochannels*, The Journal of Physical Chemistry B (2010) 132–137.

[4] Aggarwal N., Sood J., Tankeshwar K., *Anisotropic diffusion of a fluid confined to different geometries at the nanoscale.* Nanotechnology, 2007. 18(33): p. 5.

[5] Rappaport D.C., *The Art of Molecular Dynamics Simulation*, Cambridge University Press, (2004).

[6] MacKerell Jr A., et al., *CHARMM: The Energy Function and Its Parameterization with an Overview of the Program*, J. Phys. Chem. B, 102(18), 3586-3616 (1998).

[7] Ziemys A., Ferrari M., Cavasotto C. N. *Molecular Modeling of Glucose Diffusivity in Silica Nanochannels*. J. Nanosci. Nanotechnol. 2009, *9*, 6349–6359.

[8] Phillips J. C., Braun R., Wang W., Gumbart J., Tajkhorshid E., Villa, E., Chipot, C., Skeel, R. D., Kale´ L., Schulten K., *Scalable molecular dynamics with NAMD*. J. Comput. Chem. 2005, *26*, 1781–1802.

[9] Jorgensen W. L., Chandrasekhar J., Madura J. D., Impey R. W., Klein, M. L., *Comparison of simple potential functions for simulating liquid water*. J. Chem. Phys. 1983, *79*, 926–935.

[10] Cruz-Chu E. R., Aksimentiev A., Schulten K., *Water-silica force field for simulating nanodevices*. J. Phys. Chem. B 2006, *110*, 21497–21508.

[11] Gladden J.K., Dole M., *Diffusion in supersaturated solution-II: glucose solutions.* J. Am. Chem. Soc., 1953. 75: p. 3900-3904.

[12] Bathe K.J., *Finite Element Procedures*. Prentice-Hall, Inc., Englewood Cliffs, N.J., (1996).

[13] T. Hughes, *The finite element method: linear static and dynamic finite element analysis*. 2000, New York: Dover Publications.

[14] Kojic, N., A. Kojic, and M. Kojic, *Numerical determination of the solvent diffusion coefficient in a concentrated polymer solution.* Communications in Numerical Methods in Engineering, 2006. 22(9): p. 1003-1013.

[15] Kojic M., Filipovic, N., Stojanovic, B. and Kojic N. (2008), *Computer Modeling in Bioengineering*, Theoretical Background, Examples and Software, J Wiley and Sons, Chichester.

[16] Kojic M., Milosevic M., Kojic N., Ferrari M., Ziemys A., *On diffusion in nanospace*, JSSCM, Vol. 5 / No. 1, 2011 / pp. 84-109.

[17] Griess, G. A., Guiseley, K. B. & Serwer, P. The relationship of agarose gel structure to the sieving of spheres during agarose gel electrophoresis. *Biophysical Journal* **65**, 138-148 (1993).

[18] P.D. Yurchenco and G.C. Ruben, *The Journal of cell biology*, 1987, **105**, 2559-2568.

[19] R. Timpl, H. Wiedemann, V. Delden, H. Furthmayr, and K. Kuhn, *European Journal of Biochemistry*, 1981, **120**, 203-211.

[20] M. Van der Rest and R. Garrone, *The FASEB journal*, 1991, **5**, 2814-2823.

[21] G. Laurie, C. Leblond, and G. Martin, *The Journal of cell biology*, 1982, **95**, 340-344.

[22] Nicolas M. O., Oden J. T., Vemagantia K. and Remacle, *Simplified methods and a posteriori estimation for the homogenization of representative volume elements*, J. F., Comput. Methods Appl. Mech. Engrg. 176, 265-278 (1999).

[23] Chapman S. J., Shipley R. J., Jawad R., *Multiscale modelling of fluid flow in tumours*, Bull. Math. Biology 70, 2334–2357 (2008).

[24] Yu W., Tnag T., *Variational asymptotic method for unit cell homogenization of periodically heterogeneous materials*, Int. J. Solids Struct. 44 (22-23), 7510–7525 (2007).